Title
REACTION OF SILICATE GLASSES AND MULLITE WITH HYDROGEN GAS

Authors
Tso, S.T.
Pask, J.A.

Publication Date
1982-04-01

LBL-12882
Preprint

Lawrence Berkeley Laboratory
UNIVERSITY OF CALIFORNIA

Materials & Molecular Research Division

To be published in the Journal of the American Ceramic Society

REACTION OF SILICATE GLASSES AND MULLITE WITH HYDROGEN GAS

Stephen T. Tso and Joseph A. Pask

April 1982

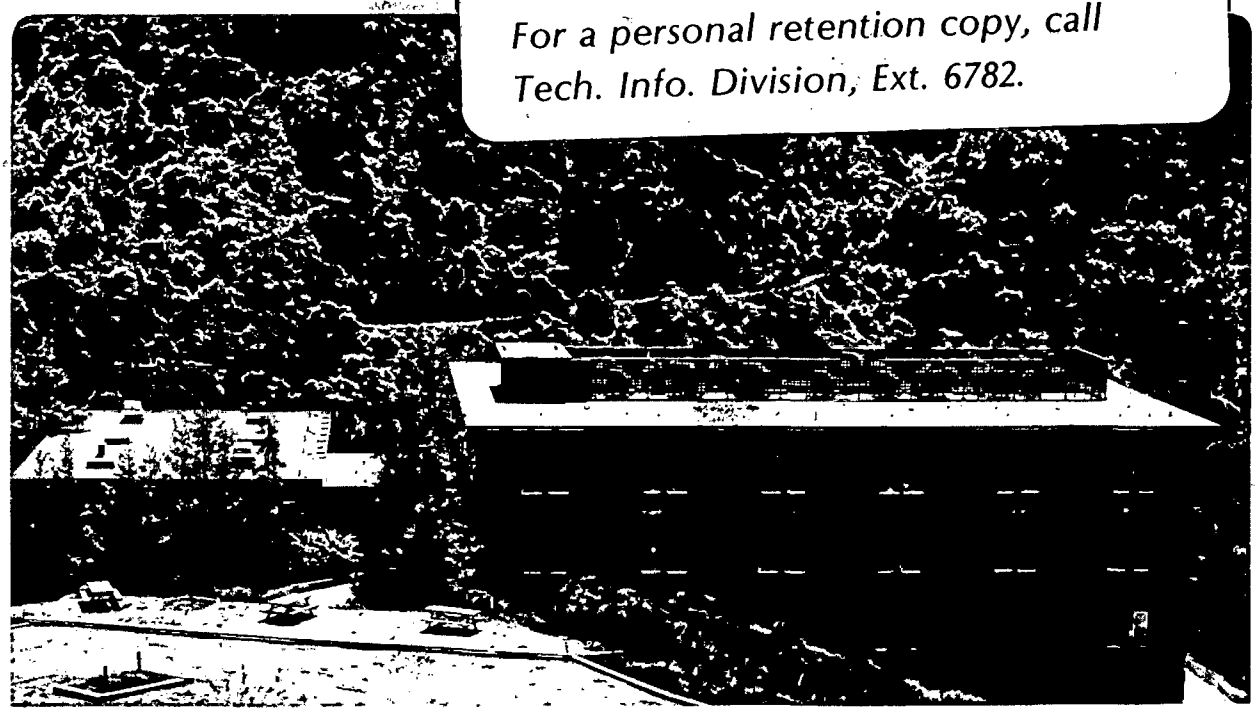

Prepared for the U.S. Department of Energy under Contract DE-AC03-76SF00098

DISCLAIMER

REACTION OF SILICATE GLASSES AND MULLITE WITH HYDROGEN GAS

Stephen T. Tso* and Joseph A. Pask

Materials and Molecular Research Division, Lawrence Berkeley Laboratory
and Department of Materials Science and Mineral
Engineering, University of California
Berkeley, CA 94720

ABSTRACT

The increasing order of corrosion resistance to flowing H_2 gas is fused silica, alumino-silicate glass, and mullite in the range of 1300 to 1500°C; the activation energies are 83.0, 85.7 and 93.0 kcal/mole (347.3, 358.6 and 389.1 kj/mole), respectively. No detectable reaction with α-Al_2O_3 was observed. Addition of a small amount of CaO to the glass reduced its activation energy (67.8 kcal/mole or 283.7 kj/mole) and made its reactivity with H_2 similar to that of mullite at elevated temperatures. The reaction product for the glasses consisted of a porous zone composed of an intermediate layer close to mullite in composition and an outer layer of α-Al_2O_3. The reaction product for mullite consisted of a porous α-Al_2O_3 residue layer.

This work was supported by the Director, Office of Energy Research, Office of Basic Energy Sciences, Materials Science Division of the U.S. Department of Energy under Contract No. DE-AC03-76SF00098.

---

*Now with Central Research Lab., Texas Instruments, Dallas, Texas.

I. INTRODUCTION

In the coal gasification reactor, refractory materials capable of withstanding corrosion by reducing atmospheres rich in hydrogen, methane, carbon monoxide and water vapor are necessary. Alumino-silicate type of refractories are most attractive economically. They have a complex microstructure containing a glassy phase and mullite. Therefore, the reactions of silicate glasses and mullite with hydrogen gas were studied to contribute to an understanding of the nature and mechanisms of the reactions. Studies of the reaction of silica glass with H_2 will be reported elsewhere[1].

II. EXPERIMENTAL

A hydrogen furnace was built for corrosion testing. The furnace design and the hydrogen flow rate were adjusted so that the total reaction rate was nominally constant and independent of the flow rate, as previously described[1]. The hydrogen gas† had a reported purity of 99.999% and a dew point of -84.4°C. The glasses* listed in Table 1, as L and S, which were used for kinetic studies, were received as slabs. They were core drilled into 9 mm diameter cylinders and then cut into 2 mm thick discs. The as-cut glass samples were treated with hydrofluoric acid solution to remove the irregularly abraded surface layers[2]. After this treatment, the glass samples were stored in a desiccator.

---

†Lawrence Berkeley Laboratory.

*Supplied by George H. Beall, Corning Glass Works.

The mullite samples were prepared by cold pressing mullite powder containing 73 wt% Al_2O_3 into discs 10 mm diameter and 2 mm thick. After sintering in air at 1600°C, the diameter was ~ 9 mm. The specimen was essentially theoretically dense with no open porosity because of the presence of a glassy phase at the grain boundaries.

The surfaces of the reacted samples were examined by an optical microscope and a scanning electron microscope. X-ray diffraction analysis was used to identify the presence and nature of crystalline phases. Chemical composition and concentration profiles were determined by electron microprobe analyses of samples that were vacuum-mounted with epoxy and polished to a quarter micron grade. The concentration profile was obtained by traversing the electron beam of ~ 1 μm diameter perpendicular to the reaction interface. If large fluctuations were present due to either phase separation or porosity, line scanning of ~ 50 to 100 μm parallel to the reaction interface was applied at every point to obtain an average composition. The data were corrected for absorption, fluorescence, atomic number, dead time, drift and background.

III. RESULTS AND DISCUSSION

(A) Reaction with Silicate Glasses

(1) Phase Separation and Crystallization of Glasses

For the alumino-silicate glass L, phase separation which can be a precursor to crystallization can occur due to a metastable immiscibility gap in the system. Crystallization was reported[3] to occur upon heating above 1000°C. Usually, the

crystalline grains remained very small so that the sample was still translucent to transparent. XRD analysis at 1200°C for 10 h indicated only mullite; after an additional 10 h at 1300°C cristobalite was also present.

For the calcium-alumino-silicate ternary glass S, the metastable immiscibility gap between SiO_2 and Al_2O_3 may be enhanced with additions of CaO since phase separation and crystallization has been observed to occur more readily in this system. The glass became opaque upon heating above 1000°C. Strong XRD peaks were observed after 10 h of heating at 1200°C, and subsequent heating at 1300°C for 10 h did not introduce significant changes to the diffraction pattern although a small increase in bulk density was monitored. In addition to diffraction peaks for mullite, a set of sharp, reproducible peaks were also present which were not definitely identified. No cristobalite peaks were found.

(2) Surface Morphology of Reacted Glasses

As hydrogen gas reacts with the multicomponent glasses to form volatile products, alumina is left behind as a residue layer which was identified as α-Al_2O_3. The surface morphology on this layer varies. For L glass, "rosettes" formed on the Al_2O_3 layer at 1350°C after reaction with hydrogen gas, as shown in Fig. 1; these did not appear in the 1500°C heating. The formation of the rosette pattern is related to the cristobalite phase[3]. As cristobalite crystallization normally occurs with a spherulitic habit and its reaction rate with hydrogen gas is slightly higher, a depression in the shape of a rosette is formed. At 1500°C, the surface diffusion rate is

higher than the reaction rate and a much smoother surface results.

For S glass, in the absence of cristobalite formation, rosette morphology was not observed on the Al_2O_3 residue layer. The observed surface morphology is shown in Fig. 2. Even at 1500°C, the α-Al_2O_3 residue agglomerate size is very small, indicating that the original mullite crystal size was small.

(3) Reaction with Flowing Hydrogen Gas

The silicate glasses devitrified to some extent on heating to the reaction temperature. Since these specimens are not single-phase homogeneous materials, kinetic studies are difficult. However, weight loss measurements were carried out to reveal the effect of composition on the corrosion resistance to hydrogen. The reaction rates of L and S glasses at 1400°C are shown in Fig. 3. The weight loss rate within the experimental range of 6 h was found generally linear with time, indicating that the porous Al_2O_3 layer was not an effective transport barrier to H_2 or reaction products.

The total reaction rate of L glass is much lower than that for pure silica glass[1], which is included in Fig. 3 for comparison. Silica glass was shown to react with H_2 to form SiO and H_2O gases, according to Eq. (1), which were carried away

$$SiO_2(s) + H_2(g) = SiO(g) + H_2O(g) \qquad (1)$$

by the flowing hydrogen leaving no residue layer. The rate-limiting step was deduced to be the desorption of the product from the glass surface[1]. If it is assumed that the same reaction takes place in L glass and that the Al_2O_3 does not react with H_2, the decrease in

reaction rate is much greater than that expected from a SiO_2 weight ratio consideration. Since the reaction rate of cristobalite with H_2 was observed to be quite comparable to that for SiO_2 glass, the small amount of crystallization of cristobalite and mullite cannot explain the reduced rate. It is thus concluded that the added Al_2O_3 helps to stabilize the SiO_2 toward reaction with H_2 gas.

The following is a possible explanation for this behavior drawn on the studies of the petroleum industry, which uses alumino-silicates as catalysts for cracking. Their structure may be viewed as tetrahedrally coordinated Si and Al atoms linked through the sharing of oxygen atoms at the corners of SiO_4 and AlO_4 tetrahedra. For Al- containing tetrahedra bonded at all four corners to Si atoms there is an excess negative charge. A compensating positive charge must be present to provide electroneutrality for the trivalent Al atom. A proton coordinated to the structure satisfies this requirement, as shown schematically in Fig. 4(a), at lower temperatures. Heating to an elevated temperature leads to a new structure, as in Fig. 4(b); the Al atom in this state is unsaturated and can serve as an acceptor for a pair of electrons, functioning as a Lewis acid site. This structure provides an explanation for the strong affinity of water vapor or hydroxyl radical to the alumino-silicate material. In the reaction with hydrogen gas, the increased interactions with the hydroxyl radical and water vapor tend to make the desorption an even slower step, thus stabilizing the silica and reducing the total reaction rate.

The addition of CaO (S glass) did not have a significant effect on the reaction rate at 1400°C, as seen in Fig. 3. However,

the reaction rate was less than that for L glass, but it was higher at 1200°C, as seen in Fig. 5. The activation energy is thus less for S glass (67.8 kcal/mole or 283.7 kj/mole) than for the other materials which have about the same value (SiO_2, 93.0; L glass, 85.7; and mullite, 93.0 kcal/mole or 347.3, 358.6 and 389.1 kj/mole, respectively).

(4) Concentration Profiles of Reacted Silicate Glasses

Cross-sections of two L glass specimens reacted at 1400°C are shown in Fig. 6A; the specimen on the right clearly shows the unreacted core with a reaction zone made up of two layers which are separated. The concentration profile perpendicular to the interfaces of a reacted zone (Fig. 7) shows that two layers are present in the reaction zone. In the figure, the distance from 0 to 23 μm marks a portion of unreacted core, 44 to 260 μm the transition layer, and 270 to 330 μm the surface Al_2O_3 layer. The distances 23 to 44 μm and 260 to 270 μm correspond to cracks between the layers while the dip around 100 μm is the result of a small pit on the sample surface.

Both the transition and the outer Al_2O_3 layer are porous, as evidenced by the fact that during the polishing process the color of diamond grit was absorbed into the surface of these layers. Furthermore, during the coating process the carbon did not adhere due to the evaporation of the absorbed polishing oil. The carbon adhered to the surface of vacuum mounted samples whose profile data were obtained by electron probe microanalysis. These pores or channels are extremely small. No pore structure could be observed by SEM. Moreover, the Al_2O_3 reading in the transition layer showed little fluctuation, indicating that the pore size is much smaller than the electron beam size so that an average

value was always obtained. The electron beam size is of the order of 1 μm implying that the pore sizes are of the order of 100 A^o or less.

In Fig. 7, the SiO_2 concentration drops abruptly at each of the interfaces (at ~ 33 μm and ~ 265 μm), suggesting that there are at least two kinds of silicate structures with different stabilities and thus with different reaction rates. The normalized weight percent of 71 wt% Al_2O_3 at the inner edge in contact with glass and 77 wt% Al_2O_3 at the outer edge of the transition layer in contact with the surface α-Al_2O_3 layer correspond to the mullite solid solution range[4]. However, it was not possible to confirm the mullite structure by XRD. The thickness of the transition layer increased with total reaction time which was due to a lower reaction rate of H_2 with mullite than with glass. At the outer edge of the transition layer the silica concentration drops to zero, since the only phase is α-Al_2O_3. The fluctuation of readings in the α-Al_2O_3 layer suggests non-uniform sintering during the reaction run.

The cross-section concentration point profile of the reacted S glass was considerably more erratic in comparison with that for the L glass. The larger fluctuations for the S glass apparently were due to the phase separation which is of a size comparable to that of the electron beam and in some cases larger. Therefore, a line scan parallel to the reaction interfaces was performed at fixed distances and the profile thus obtained is shown in Fig. 8. In this averaged profile it can be seen that similar layers were formed as in the L glass. From left to right, these layers as determined by the Si and Al profiles are unreacted core (up to ~ 22 μm), the overall transition layer (~ 22 to

~ 250 μm), and the alumina layer (beyond ~ 250 μm). The Ca profile remains essentially constant in the transition layer but disappears together with the SiO_2 in the outer Al_2O_3 layer whose thickness is not shown in the overall profile. As CaO is not expected to react with hydrogen gas, according to thermodynamic data, it should be left behind as a residue with the Al_2O_3. Its absence in the outer layer suggests that at some decreasing SiO_2/Al_2O_3 ratio, CaO becomes available to react with water vapor which is formed as a product of the H_2 reaction with SiO_2. Further study is needed to ascertain the mechanism and kinetics.

(B) Reaction with Mullite

Since preliminary corrosion tests showed that mullite reacted with hydrogen gas and that the small amount of glassy phase along grain boundaries had a minimal effect on the reaction rate, the effect of compositional and microstructural variations in the mullite specimens was not determined. The cross-section of the mullite sample reacted at 1400°C is shown in Fig. 9. The overall cross-section is shown at low magnification, Fig. 9A; the central strip is the unreacted mullite core. A high magnification of a section of the right interface showing the reacted layer is shown in Fig. 9B. It can be seen that the reaction front is flat within a few microns. The composition profile of the cross-section across the reacted surface layer showed no transition layer in contrast to the glasses with lower Al_2O_3 contents. The silica concentration in the mullite at the interface drops to zero in the α-Al_2O_3 reaction layer.

The weight loss per unit surface area vs time for

reactions with H_2 at temperatures from 1350 to 1500°C is plotted in Fig. 10. The linear relationship indicates that, within the experimental conditions, the alumina residue remains porous and that the transport of reactant and products through this layer is not the rate limiting step. Furthermore, the composition profile suggests that the reaction is rate limiting. The 1400°C curve of Fig. 10 plotted in Fig. 3 and the Arrhenius plot of the Fig. 10 data in Fig. 5 provide a comparison of the mullite reaction rate with those for fused silica and the experimental glasses. The activation energy of 93.0 kcal/mole (389.1 kj/mole) for mullite is close to that for silica glass and alumino-silicate glass. The presence of CaO in the alumino-silicate glass lowers the activation energy; as a result, the reactivity of this type of glass appears to be similar to mullite at higher temperatures.

(C) Character of Reacted Zones

The cracks in the reacted glass samples tend to follow the interfaces as observed in the right specimen of Fig. 6A. The adherence between the unreacted core and the transition layer appears to be better in the left specimen. A higher magnification (Fig. 6B) of the portion inside the square in Fig. 6A, however, reveals a crack at the interface as indicated by a bright strip on the sample due to the charging effect on observation by SEM. The concentration profile of the cross-section in Fig. 7 also supports this observation. In the case of reacted mullite, on the other hand, the cracks go through the reaction interface (Fig. 9) indicating good interfacial adherence between the reacted and unreacted layers.

In all cases, the residue Al_2O_3 layer remains porous and

does not halt the reaction. If the Al_2O_3 layers could be sintered into a dense layer, they may act as protective layers. Reacted samples were thus heated to 1600°C for 4 h in air. With alumino-silicate glass, the sintered Al_2O_3 layer cracked into pieces and adhered poorly due to differences in thermal expansion coefficients. With calcium-alumino-silicate glass, a liquid phase formed and rod-shaped mullite grains (confirmed by EDAX) were found growing on the surface.

Because of mullite's greater refractoriness, reacted mullite specimens were sintered at 1650 and 1700°C as well as 1600°C. Sintering of the alumina layer was achieved in all of these firings, but cracks were present on observation of the surface by SEM at room temperature. The nature of the cracks, shown in Fig. 11, suggest that cracking occurred on cooling. Further efforts in this direction were not pursued.

IV. SUMMARY

For alumino-silicate (L) and calcium-alumino-silicate (S) glasses, phase separation and crystallization occurred at elevated temperatures ($\gtrsim$ 1000°C). After reaction with H_2 gas, the reaction zone consisted of two layers: an intermediate transition layer with a SiO_2 content similar to that of mullite, and an outer α-Al_2O_3 residue layer free of SiO_2. Both of these layers were porous. Mullite on reaction with H_2 gas had only one reaction layer consisting only of α-Al_2O_3. The order of decreasing reactivity with H_2 is fused SiO_2, alumino-silicate glasses, mullite and α-Al_2O_3. The addition of small amounts of CaO to the glasses had little effect, but the reactivity of the glasses approached that of

mullite at higher temperatures because of a smaller activation energy. The reaction layers were porous and did not retard the reaction rates under the experimental conditions of the study indicating that the reaction was the slow step of the overall corrosion process. Sintering of the Al_2O_3 surface layer did not result in a protective layer because of the presence of surface cracks at room temperature which appear to have been formed on cooling. It is of interest to note that in the case of hydrofluoric acid corrosion multicomponent glasses have lesser resistance than SiO_2 glass.[2]

ACKNOWLEDGMENT

The support of the Division of Materials Research of the National Science Foundation under Grant No. DMR 79-16891-ZF is gratefully acknowledged. This work was also supported by the Director, Office of Energy Research, Office of Basic Energy Sciences, Material Sciences Division of the U.S. Department of Energy under Contract Number DE-AC03-76SF00098.

REFERENCES

1. S. T. Tso and J. A. Pask, "Reaction of Fused Silica with Hydrogen Gas," to be published.
2. S. T. Tso and J. A. Pask, "Reaction of Glasses with Hydrofluoric Acid Solution," to be published.
3. J. F. MacDowell and G. H. Beall, "Immiscibility and Crystallization in Al_2O_3-SiO_2 Glasses," J. Am. Ceram. Soc., 52 [1] 17-25 (1969).
4. I. A. Aksay and J. A. Pask, "Stable and Metastable Equilibria in the System SiO_2-Al_2O_3," J. Am. Ceram. Soc., 58 [6] 507-512 (1975).

TABLE I

GLASSES	WT. PERCENT			MOLAR PERCENT			DENSITY
	SiO_2	Al_2O_3	CaO	SiO_2	Al_2O_3	CaO	
Silica	100	0	0	100	0	0	2.20
L	70	30	0	79.8	20.2	0	2.42
S	57.1	38.1	4.8	67.5	26.5	6.0	2.52

FIGURES

Fig. 1. Surface morphology of L glass after reaction with flowing H_2 gas at 1350°C.

Fig. 2. Surface morphology of S glass after reaction with flowing H_2 gas at 1500°C.

Fig. 3. Total reaction rates of flowing H_2 with SiO_2 glass, L and S glasses, and mullite at 1400°C.

Fig. 4. Structure of aluminosilicate compound with aluminum ion bonded tetrahedrally: (a) dried at low temperature, and (b) heated to elevated temperature.

Fig. 5. Temperature dependence of total reaction rates of SiO_2 glass, L and S glasses, and mullite with flowing H_2 gas.

Fig. 6. Cross-section of L glass after reaction with flowing H_2 at 1400°C. Cracks developed along interfaces of reaction layers. Higher magnification photos of portion outlined by square in low magnification photo (a).

Fig. 7. Normalized concentration profile of L glass after reaction with flowing H_2 gas at 1400°C (see text).

Fig. 8. Normalized concentration profile of S glass after reaction with flowing H_2 gas at 1500°C. Profiles obtained by revised line scan method (see text).

Fig. 9. Cross-section of mullite after reaction with flowing H_2 gas at 1400°C. Cracks propagate across interfaces. Photos (b), (c) and (d) - higher magnifications of right interface in photo (a).

Fig. 10. Weight loss vs time for mullite from 1350 to 1500°C in flowing H_2 gas.

Fig. 11. (Top) Surface layer of mullite after reaction with flowing H_2 at 1400°C. (Bottom) Surface layer of reacted specimen showing cracks after an additional sintering in air at 1600°C.

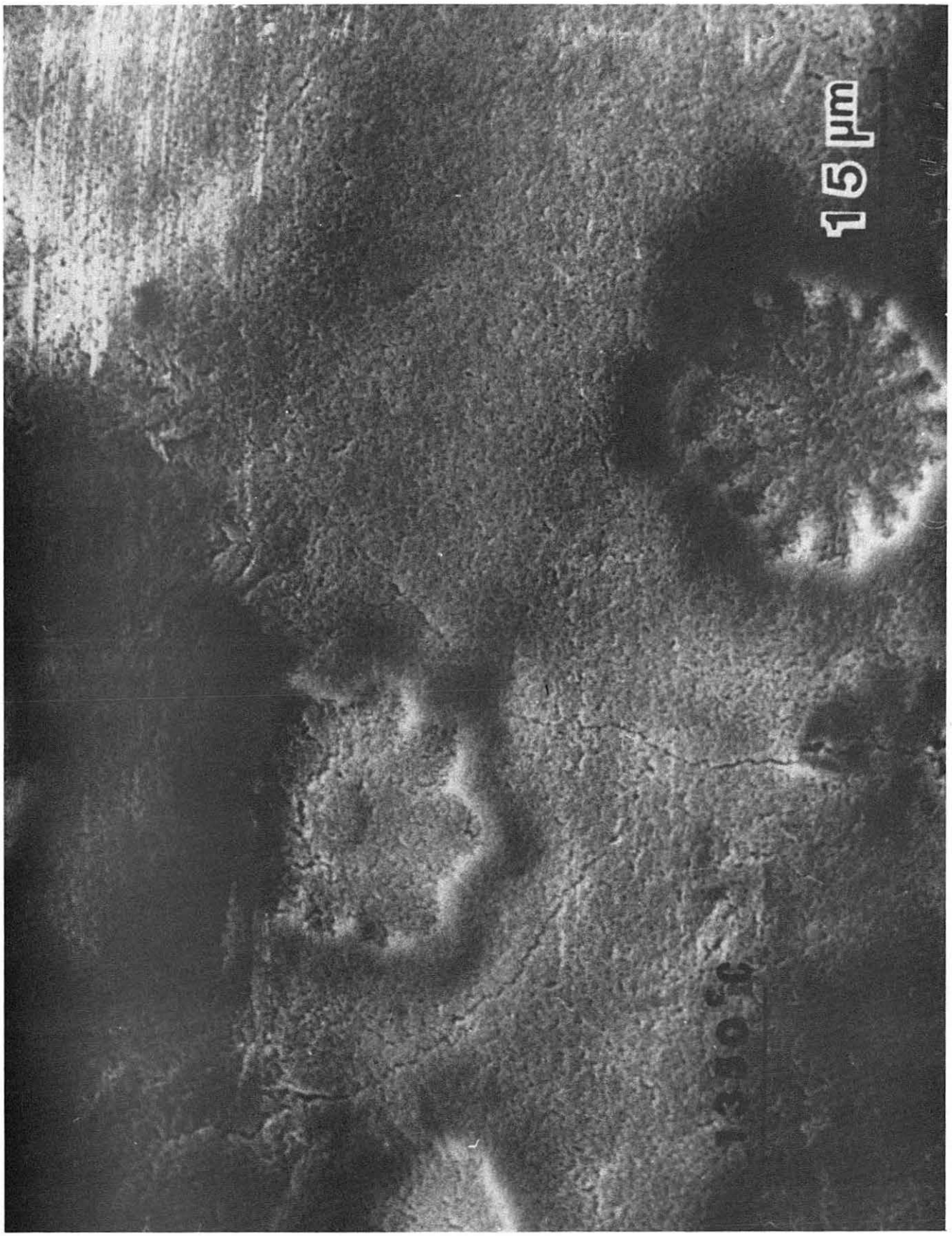

XBB794-5462

Fig. 1

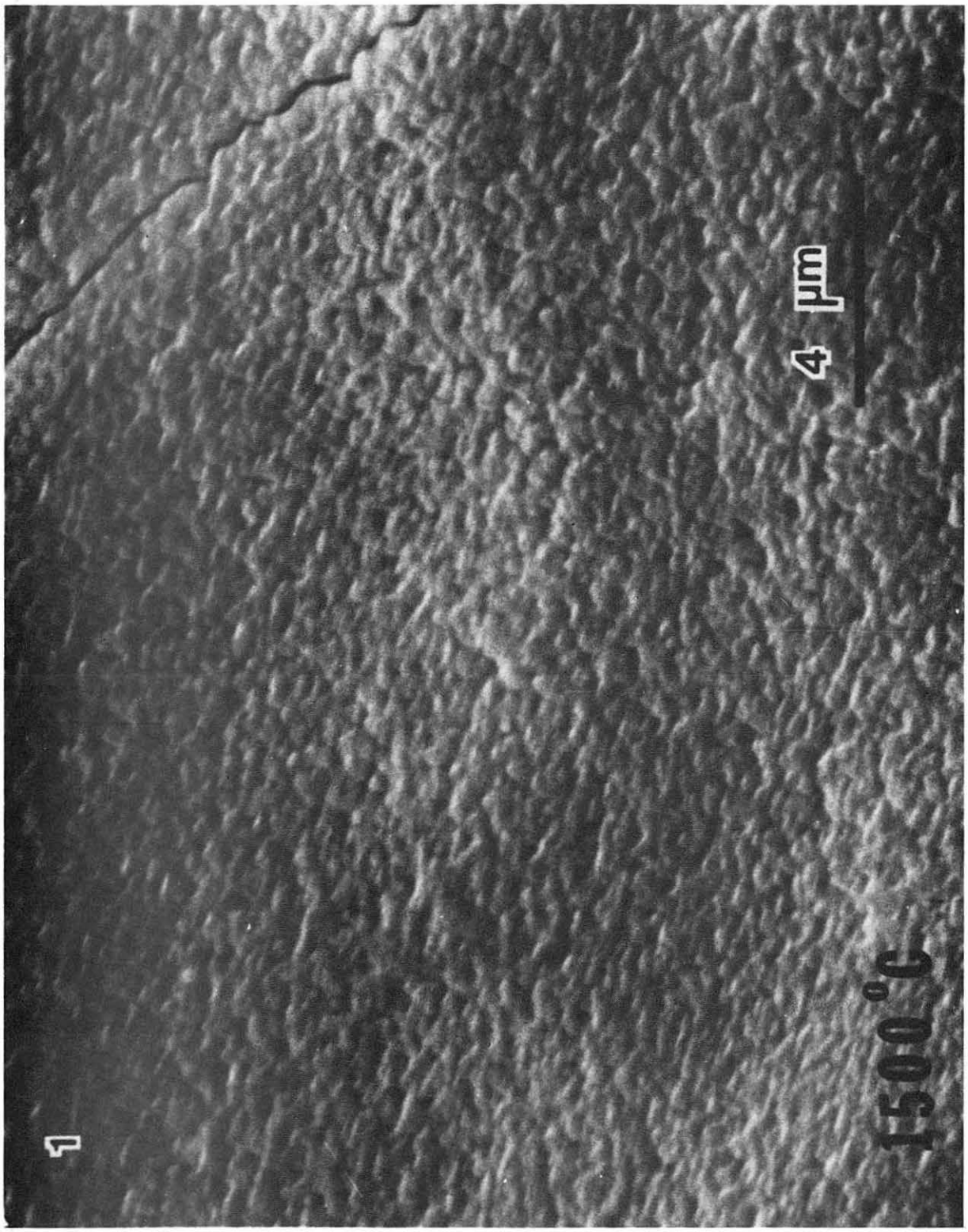

XBB797-9281

Fig. 2

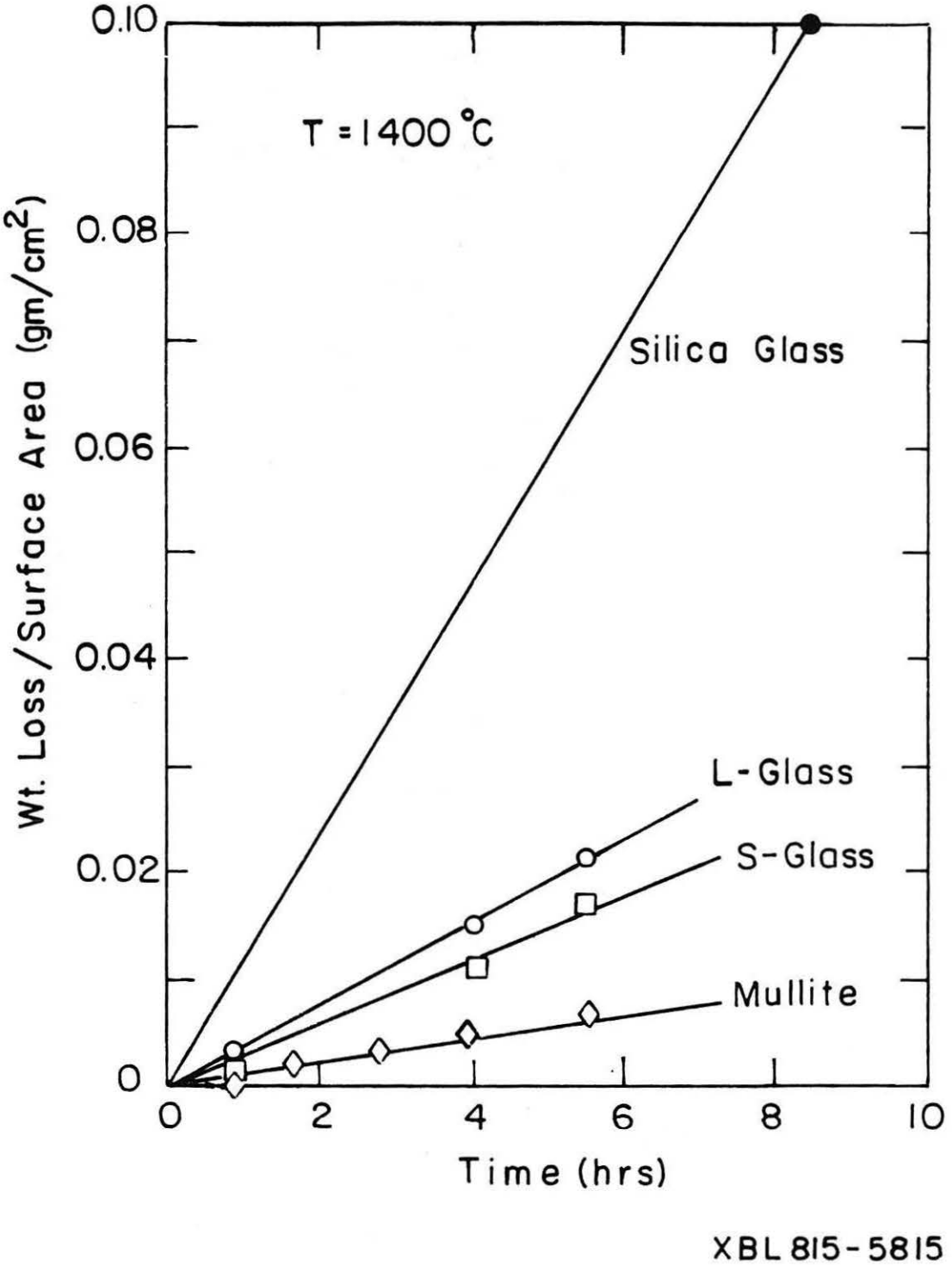
0.10
0.08
0.06
0.04
0.02
0
T = 1400 °C
Silica Glass
L-Glass
S-Glass
Mullite
Wt. Loss / Surface Area (gm/cm²)
0
2
4
6
8
10
Time (hrs)
XBL 815-5815

Fig. 3

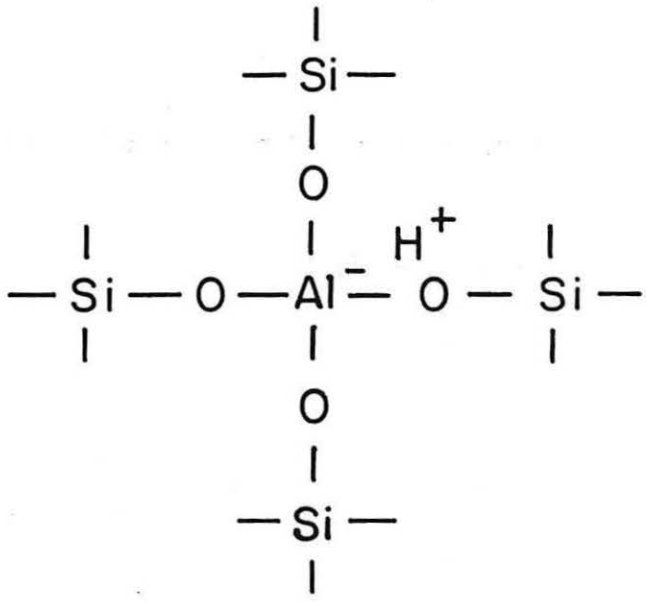

(a)

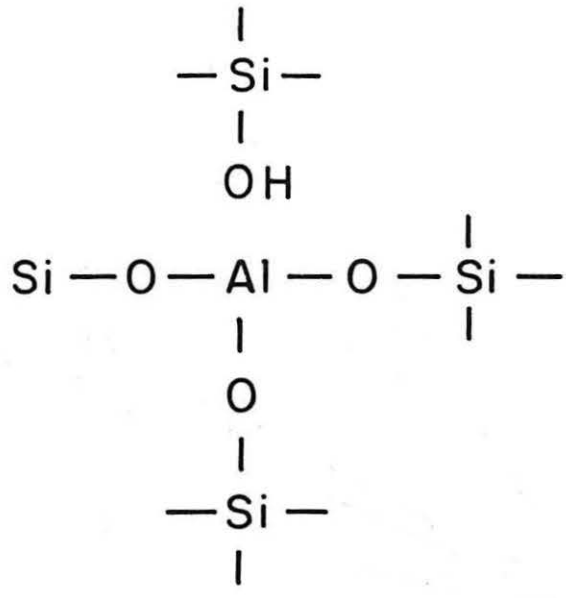

(b)

XBL799-6992

Fig. 4

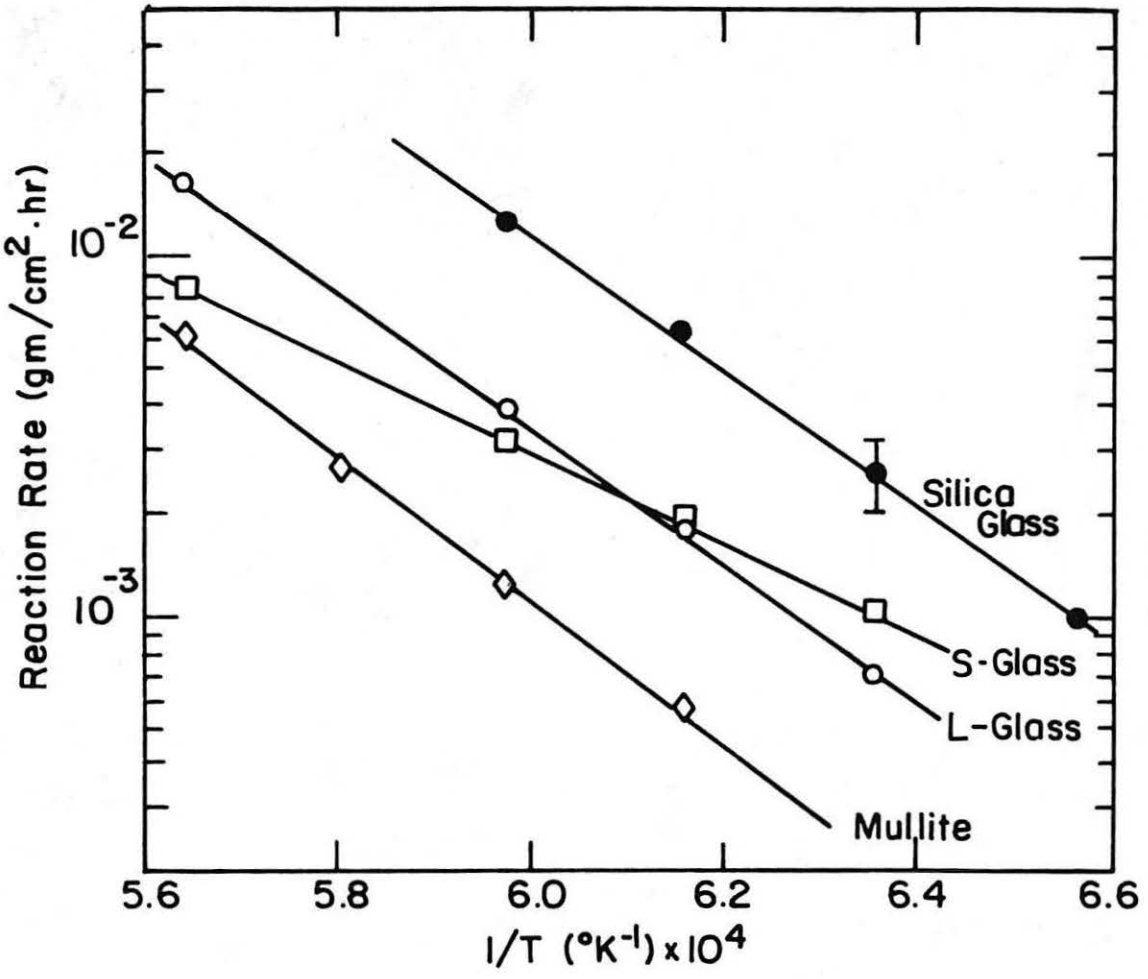

XBL 815-5816

Fig. 5

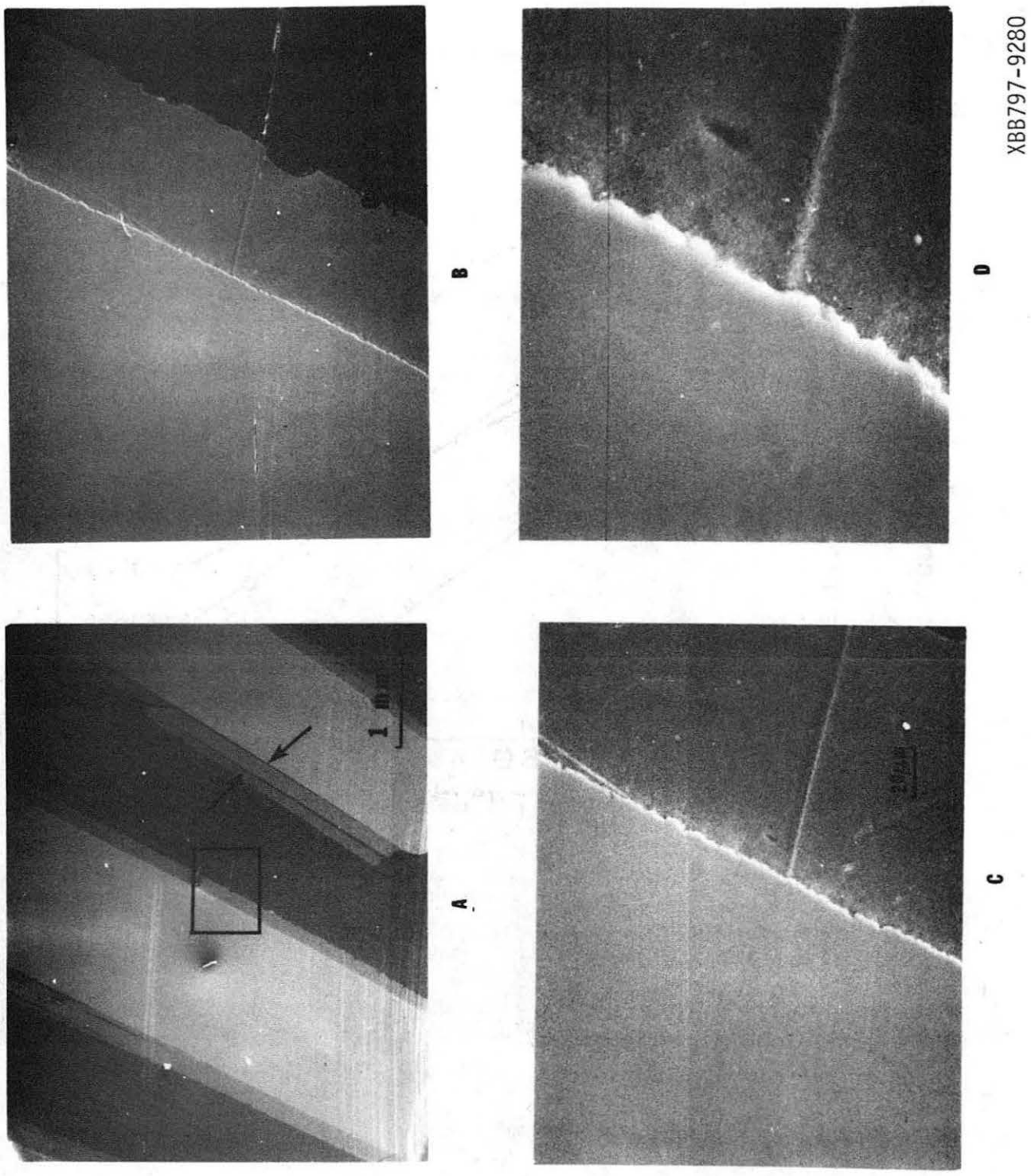

Fig. 6

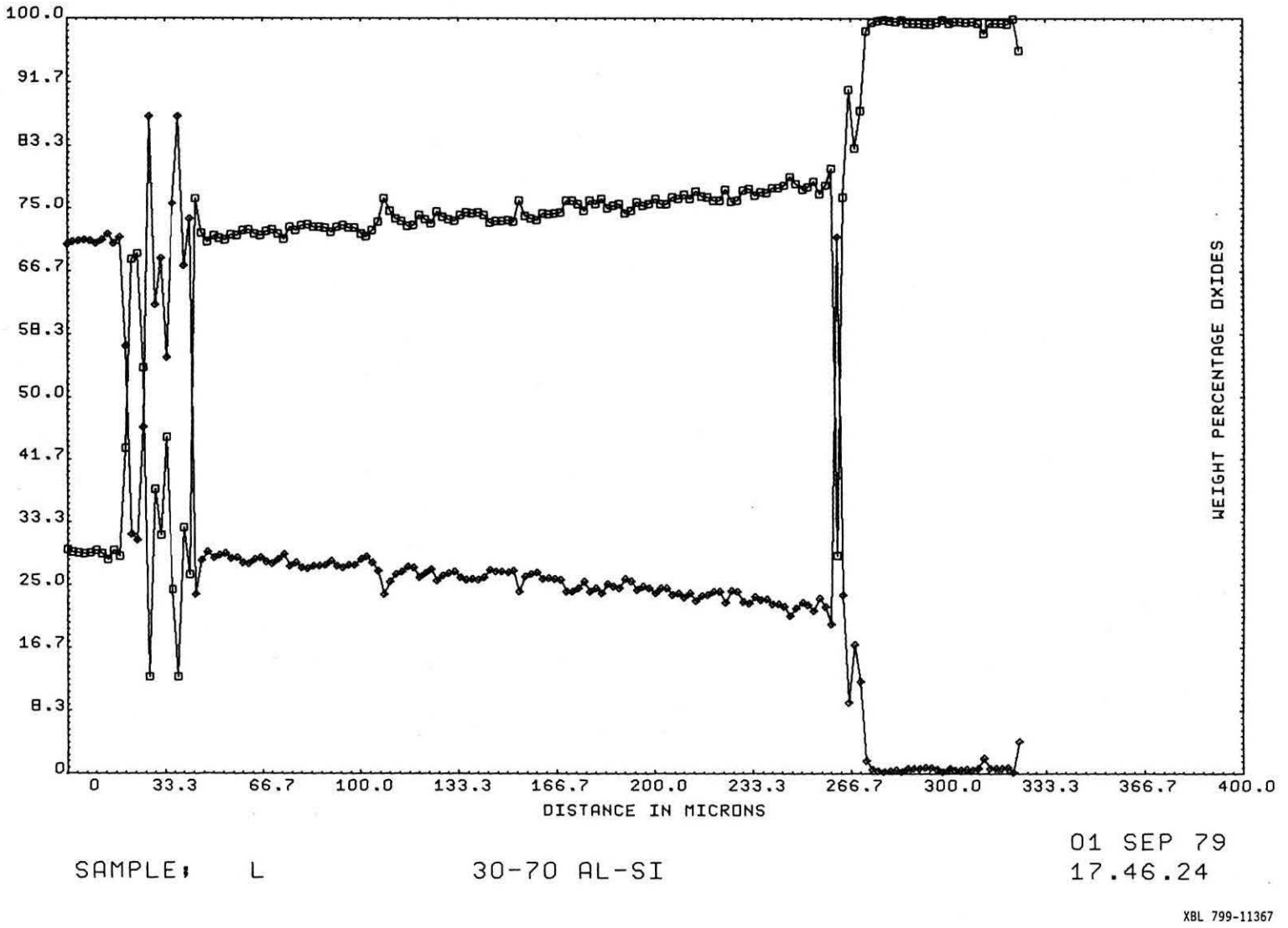
100.0
91.7
83.3
75.0
66.7
58.3
50.0
41.7
33.3
25.0
16.7
8.3
0
0
33.3
66.7
100.0
133.3
166.7
200.0
233.3
266.7
300.0
333.3
366.7
400.0
DISTANCE IN MICRONS
WEIGHT PERCENTAGE OXIDES
SAMPLE: L
30-70 AL-SI
01 SEP 79
17.46.24
XBL 799-11367

Fig. 7

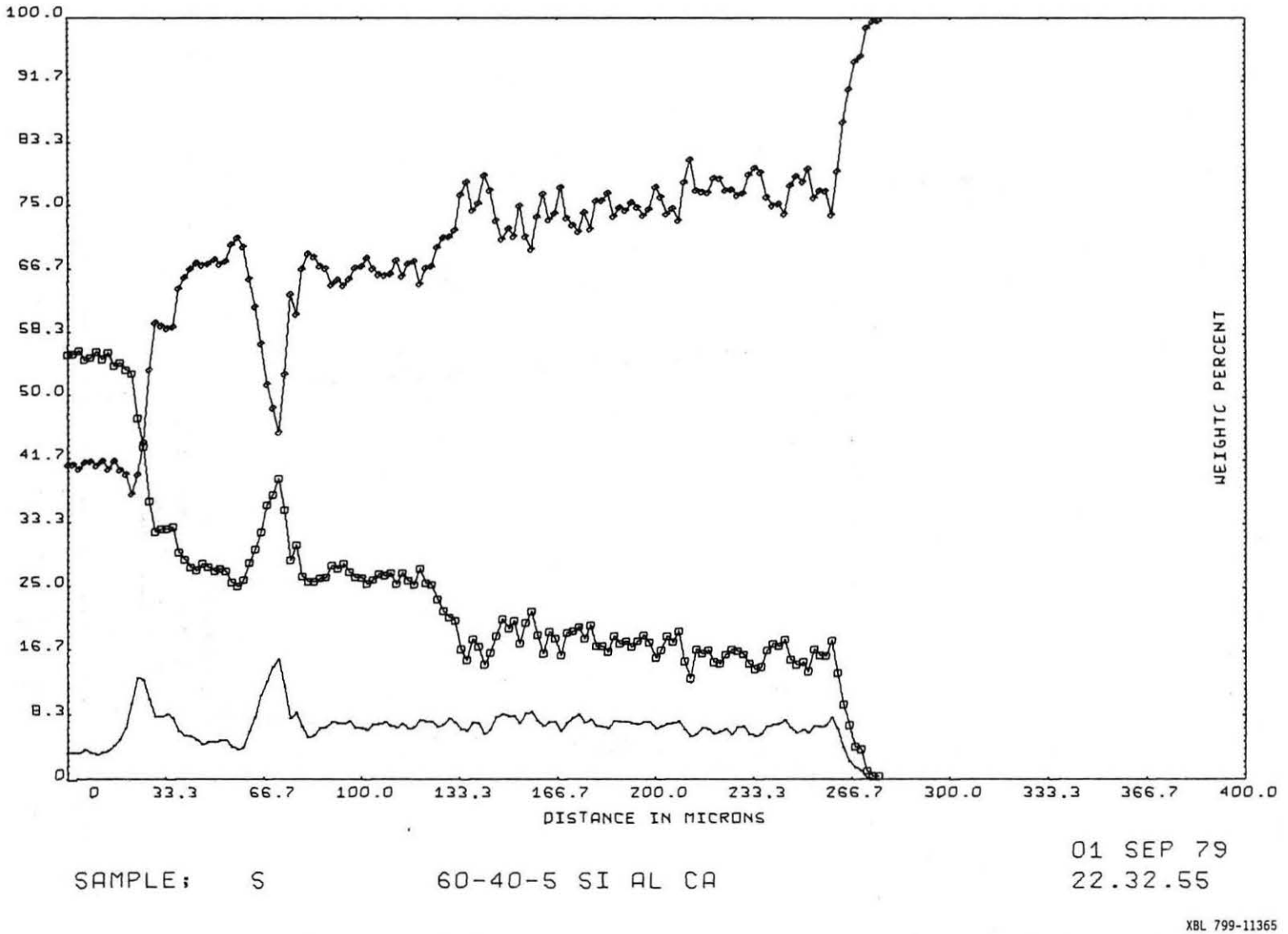
100.0
91.7
83.3
75.0
66.7
58.3
50.0
41.7
33.3
25.0
16.7
8.3
0
0
33.3
66.7
100.0
133.3
166.7
200.0
233.3
266.7
300.0
333.3
366.7
400.0
DISTANCE IN MICRONS
WEIGHTC PERCENT
SAMPLE; S 60-40-5 SI AL CA
01 SEP 79
22.32.55
XBL 799-11365

Fig. 8

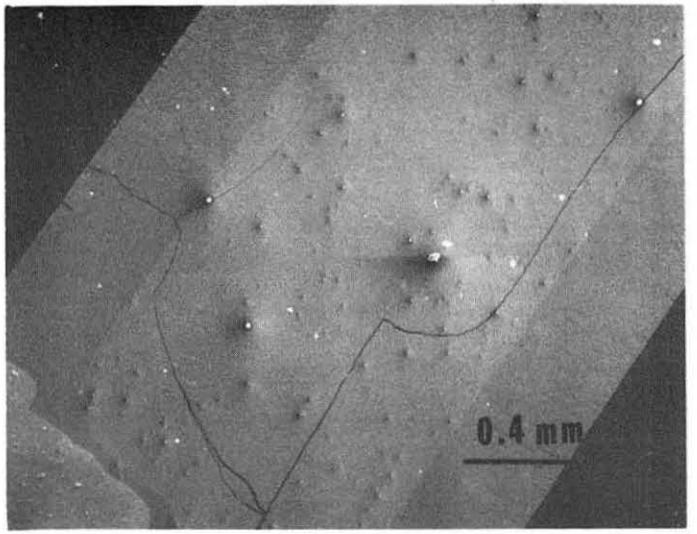

A

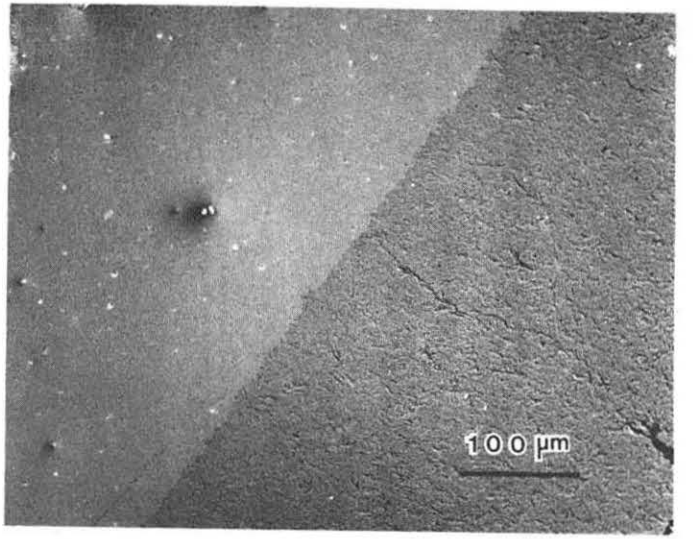

B

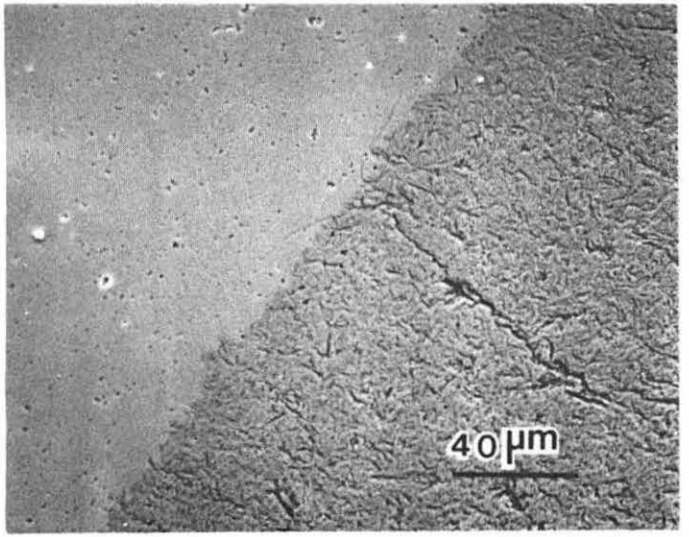

C

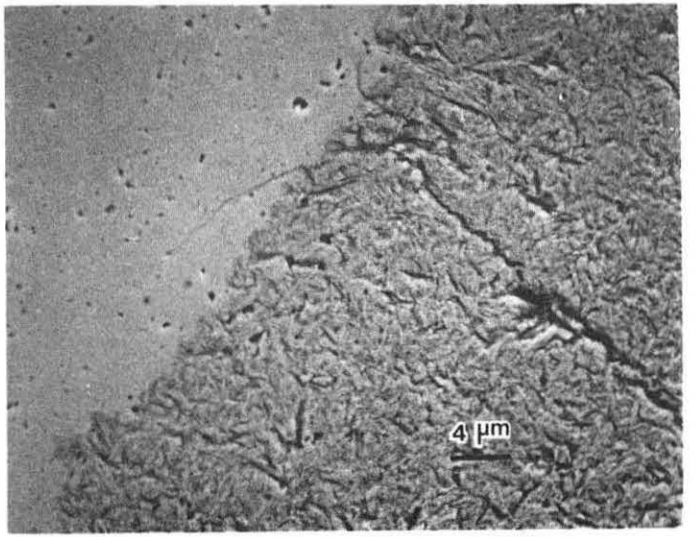

D

XBB797-9279

Fig. 9

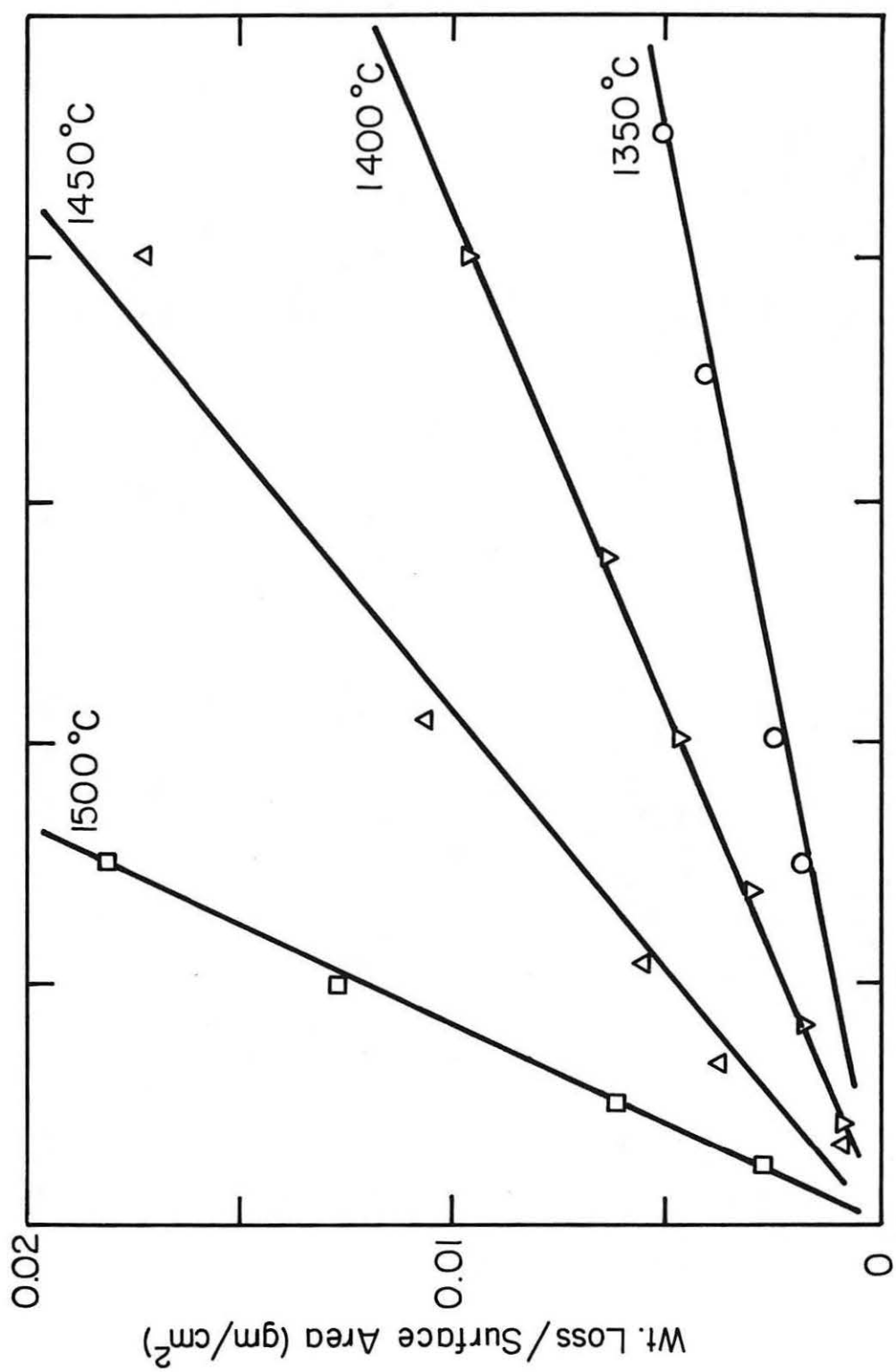

XBL 797-6548

Fig. 10

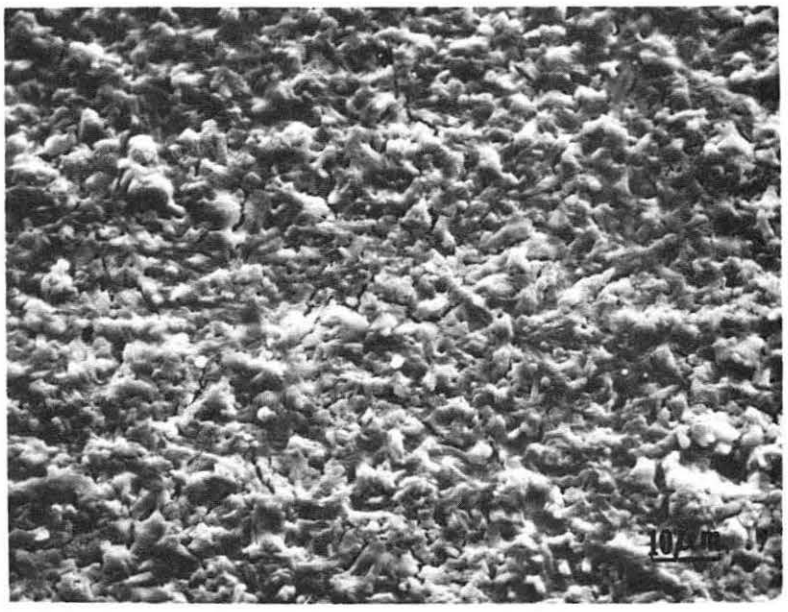

AS REACTED
1400°c

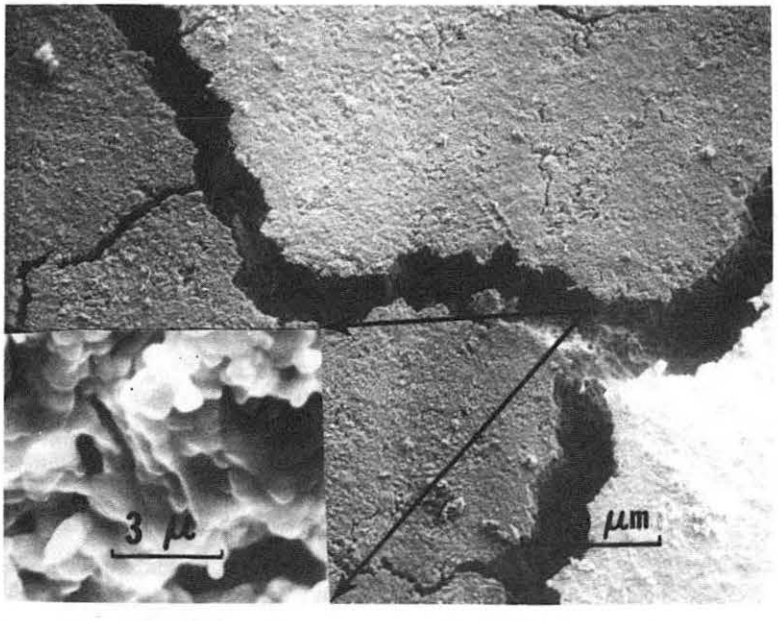

REACTED AND SINTERED
1400°c 1600°c

XBB797-8915

Fig. 11

This report was done with support from the Department of Energy. Any conclusions or opinions expressed in this report represent solely those of the author(s) and not necessarily those of The Regents of the University of California, the Lawrence Berkeley Laboratory or the Department of Energy.

Reference to a company or product name does not imply approval or recommendation of the product by the University of California or the U.S. Department of Energy to the exclusion of others that may be suitable.

TECHNICAL INFORMATION DEPARTMENT
LAWRENCE BERKELEY LABORATORY
UNIVERSITY OF CALIFORNIA
BERKELEY, CALIFORNIA 94720